

## Paramagnetic resonance hyperfine structure of hexachloroprotactinate(IV)

Ramiro Arratia-Perez and Dennis S. Marynick

*Department of Chemistry, University of Texas at Arlington, Arlington, Texas 76019-0065*

(Received 10 August 1987)

Dirac scattered-wave calculations are presented for the  $\text{PaCl}_6^{2-}$  cluster that models the  $\text{Pa}^{4+}$  impurity site in the octahedral  $\text{Cs}_2\text{ZrCl}_6$  lattice. The calculations predict a  $\Gamma_{7u}$  ground state, and show fairly good agreement with the observed  $g$  tensor,  $^{231}\text{Pa}$  hyperfine interactions, and crystal-field splittings. The Zeeman and  $^{231}\text{Pa}$  hyperfine interactions are isotropic, arising from the large orbital contributions to the magnetic moment of the ground Kramers doublet. The amount of covalency is predicted to be about 3%, and the largest contribution to covalency comes from the chlorine  $3d_{5/2}$  spinors ( $\sim 2\%$ ).

### I. INTRODUCTION

Hyperfine interactions in molecular radicals provide important information about electronic structure and chemical-bonding characteristics. For most radicals the observed tensors can be decomposed into an isotropic Fermi term and traceless spin-dipolar contributions. Radicals containing heavy atoms, however, are often complicated by orbital contributions to the Zeeman and hyperfine tensors arising from spin-orbit mixings with various excited states. Because these contributions from electronic orbital motion are neither isotropic nor traceless, one cannot make a simple decomposition of the observed hyperfine tensors into isotropic and anisotropic parts. Inorganic complexes of actinide ions are characterized as having large orbital contributions to their hyperfine tensors because the observed molecular  $g$  tensors are significantly shifted from the spin-only value of 2.0023.<sup>1,2</sup>

A crystal-field solution may be obtained by exploiting the fact that most of the unpaired spin is localized on the actinide ion. Thus, an atomic calculation of spin-orbit mixings can be made by incorporating an orbital reduction factor to simulate covalency effects.<sup>1,2</sup> Alternatively, an empirical estimate of spin-orbit mixings may be obtained from the observed molecular  $g$  tensors.<sup>3,4</sup> However, even if the spin is localized, excited states may have appreciable spin-orbit mixing to the ground state, and these are difficult to include in a crystal-field or ligand-field framework. Moreover, empirical ligand-field models that allow the relativistic atomic orbitals to mix with ligand orbitals of the appropriate symmetry are usually fit to experimental data, and in many cases there are more parameters than data.<sup>5</sup> Hence, it is important to perform calculations on actinide-ion complexes in a nonempirical fashion. In this paper we use relativistic electronic structure (four-component) calculations to analyze covalency effects and crystal-field, Zeeman, and hyperfine interactions in the  $\text{PaCl}_6^{2-}$  cluster that arises from the doping of the paramagnetic  $\text{Pa}^{4+}$  ion in a cubic lattice of  $\text{Cs}_2\text{ZrCl}_6$ .<sup>6,7</sup>

In spite of the recent advances in the development of reliable methods to calculate the electronic structure of

molecules containing heavy atoms, theoretical studies of actinide complexes represent a major challenge to conventional methods of quantum chemistry.<sup>8-12</sup> Several relativistic methods use a Pauli Hamiltonian to calculate only the large two-component of the molecular wave function. Commonly, the Darwin and the mass-velocity corrections are included in the self-consistent procedure, and the spin-orbit operator is added in a second step.<sup>11,13,14</sup> These approaches yield useful insights into the bonding and optical properties of actinide molecules; however, since they all generate only the large components of the wave function, they discard important information related to the molecular magnetic resonance behavior. Four-component theories, which use the Dirac equation as the fundamental wave equation, determine the small and the large components of the relativistic wave function. This is of fundamental importance for two reasons. First, spin-orbit effects are built into the theory so that there is no need to add these effects as perturbations. Second, as mentioned above, the small components of the wave function carry information related to the magnetic resonance behavior of molecules, particularly, their interactions with the magnetic fields.<sup>15</sup>

Dirac electronic structure calculations on actinide complexes have been mainly carried out within the framework of local-density-functional or Dirac-Slater theories, in which the wave function may be expanded in a basis set of atomiclike spinors<sup>16,17</sup> or may be determined by multiple-scattering theory.<sup>18,19</sup> In particular, both methods have been applied to the  $\text{UF}_6$  and  $\text{NpF}_6$  complexes.<sup>16-19</sup> The basis-set-expansion calculation exhibited good agreement between experimental and calculated energies for the electronic excited states of  $\text{NpF}_6$ ,<sup>16</sup> while the multiple-scattering calculation on the same complex showed good agreement between the observed and calculated  $g$  tensor and metal and ligand hyperfine interactions.<sup>19</sup>

The paramagnetic resonance spectrum of tetravalent  $^{231}\text{Pa}$  has been observed in a single crystal of  $\text{Cs}_2\text{ZrCl}_6$  at liquid-helium temperatures.<sup>6</sup> The crystal-field splittings of the  $5f$  orbitals have been measured through infrared optical absorption, and the nuclear magnetic moment of  $^{231}\text{Pa}$  was reported by Axe *et al.*<sup>7</sup> The paramagnetic re-

laxation time for the  $\text{Pa}^{4+}$  ion in the same matrix has also been determined.<sup>20</sup> Both electron-spin-resonance (ESR) and electron-nuclear double-resonance (ENDOR) spectra have been fitted to an isotropic spin Hamiltonian to provide information about the molecular  $g$  tensor and  $^{231}\text{Pa}$  hyperfine interactions.<sup>6,7</sup> Conventional molecular-orbital descriptions for hexachloroprotactinate(IV) have been obtained via a quasirelativistic spin-restricted Hamiltonian that omits spin-orbit coupling, thus preserving the single-point symmetry throughout.<sup>21</sup> However, it is shown here that quasirelativistic calculations are inappropriate for actinide complexes, because spin-orbit effects are so dominant.

Hexachloroprotactinate(IV) is an ideal system for a detailed theoretical investigation through a fully relativistic molecular-orbital formalism for the following reasons: the effects of the electrostatic crystal field are at least comparable to the spin-orbit interaction, the coupling between the magnetic electrons and the lowest excited states are known, the hyperfine structure of the paramagnetic resonance spectrum is well resolved, the symmetry of the host crystal is relatively simple, and the orbital contribution to the Kramers doublet is large.<sup>7,20</sup> Moreover, the wave functions for this system (which can be approximately described as containing a single unpaired  $5f$  electron outside the closed-shell configuration of  $\text{UF}_6$ ) should be well represented by a single determinant of Dirac spinors. Thus, the complicated intermediate coupling between the magnetic electrons of the actinide group is avoided.

## II. METHOD OF CALCULATION

The Dirac scattered-wave (DSW) method was first developed by Yang and Rabii<sup>22</sup> for calculations of bound-state wave functions, and the reader is referred to recent review for further details.<sup>23–25</sup> This method uses the Dirac rather than the Schrödinger equation to generate the one-electron orbitals. Relativistic effects such as spin-orbit interaction and Darwin and mass-velocity corrections are implicitly included at the self-consistent-field (SCF) stage. The DSW formalism incorporates two fundamental assumptions. First, the wave function is approximated as a Slater determinant of four-component molecular spinors determined by an effective Coulomb and exchange-correlation potential. Second, the molecular potential is spherically averaged inside spheres around each nucleus, and outside an outer sphere that surrounds the entire cluster. To determine the radii of these spherical cells, we followed the suggestion of Norman,<sup>26</sup> that the ratios of sphere sizes be the same as for those spheres that surround an atomic number of electrons when the atomic-charge densities are superimposed at the desired molecular geometry. This procedure gave values of 3.06 and 2.71 a.u. for Pa and Cl, respectively. The outer sphere was taken to be tangent to the chlorine spheres, with a radius of 7.48 a.u. The influence of the remaining crystalline environment was mimicked by placing a uniform charge distribution on this outer sphere to achieve neutrality in the cluster. The basis of angular-momentum functions was expanded up to  $l=4$  on the outer and Pa spheres and through  $l=2$  on Cl. Using this "extended"

basis, each iteration required about 8 s on a CRAY-XMP/24 computer, and about 35 iterations were required to achieve self-consistency. The Pa—Cl bond length at the  $\text{Pa}^{4+}$  impurity site in the  $\text{Cs}_2\text{ZrCl}_6$  lattice is not known. In pure compounds the average Pa—Cl distance is generally in the range of 2.6–2.7 Å (for example, in  $\text{PaCl}_4$  it is 2.64 Å),<sup>27,28</sup> whereas the cation-anion distance in  $\text{Cs}_2\text{ZrCl}_6$  is 2.44 Å.<sup>7</sup> Due to the uncertainty in bond length we have chosen Pa—Cl distances of 2.52 and 2.62 Å. As we show below, the bonding trends and spin distributions are fairly insensitive to this small change in bond length.

For the exchange-correlation potential, we have used the original Slater  $X\alpha$  potential in which the exchange parameter  $\alpha$  is an adjustable one,<sup>29</sup> and the Hedin-Lundqvist (HL) potential<sup>30</sup> modified to include relativistic effects.<sup>31</sup> The HL function is similar to the Slater potential, but with a density-dependent function in which the contribution to the exchange and correlation energy at each point is assumed to be the same as that in a homogeneous electron gas of the same density. Thus, the HL potential adds Coulomb correlations not present in the simplest Slater potential.<sup>30</sup> The relativistic exchange-correlation potential has been tested in atomic calculations.<sup>32</sup> It exhibits important differences from the nonrelativistic counterparts in regions of high-electron density, but is very similar in the low-electron-density regions of the valence orbitals of atoms.<sup>32</sup> We have also performed nonrelativistic limit (NRL) calculations by setting the speed of light to a very large value ( $c = 10^{15}$  a.u.) in order to estimate quantitatively the relativistic effects.

## III. RESULTS AND DISCUSSION

### A. Molecular orbitals

Figure 1 shows the molecular-orbital energies for three spin-restricted scattered-wave calculations (performed at 2.62 Å) on  $\text{PaCl}_6^{2-}$ . In column A the orbital energies as determined by the (NRL) calculation are presented, while columns B and C show the relativistic orbital energies using Slater's potential (column B) and the relativistic exchange-correlation potential (column C).<sup>31–32</sup> The valence levels of columns B and C are unchanged, except for a rigid downward shift of 0.77 eV obtained in calculation C. For all the calculations the  $5f$ -like "crystal-field" levels are the highest occupied molecular orbitals (HOMO's  $a_{2u}$  and  $2e_{3u}$ ) and those above. The symmetries of the ground-state and excited energy levels are in good agreement with the previous crystal-field analysis of the optical spectra.<sup>7</sup> The orbitals below the HOMO's are formed primarily from the chlorine  $3p$  orbitals, with some small contributions from the protactinium. For the relativistic molecular orbitals our notation is related to Bethe's notation as follows.  $e_2 = \gamma_6$ ,  $e_3 = \gamma_7$ , and  $q = \gamma_8$ . If we compare column A against column B or C we observe that relativistic effects destabilize the crystal-field orbitals and stabilize those orbitals in which the metal-ligand interactions are significant. The spin-orbit splittings of the various nonrelativistic triply degenerate orbitals are also indicated in Fig. 1 (although spin-orbit

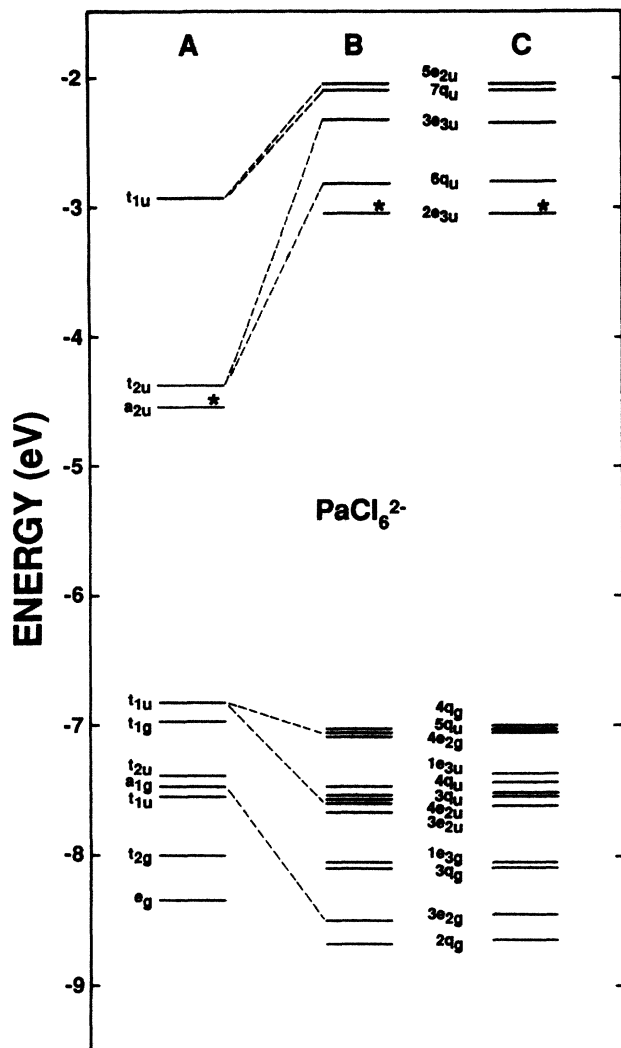


FIG. 1. Orbital energies for three spin-restricted scattered-wave calculations at the Pa—Cl distance of 2.62 Å; see the text. A: nonrelativistic limit. B: DSW calculation using Slater's potential. C: DSW calculation using the relativistic exchange-correlation potential of Refs. 30 and 31. The energies in column C have been uniformly shifted up by 0.77 eV to facilitate comparison with column B. The highest occupied orbital is marked with an asterisk in each case.

effects couple levels together, to a good approximation, each can be treated as if it were derived from a single-parent orbital). Among the fully occupied energy levels, the nonrelativistic  $t_{1u}$  level splits by about 0.6 eV due to spin-orbit interaction involving the  $7p_{1/2}$ - $7p_{3/2}$  spinors. This splitting is smaller than the calculated splitting in  $\text{NpF}_6$  (about 1.1 eV),<sup>16,19</sup> probably due to a larger participation of the chlorine orbitals in this level. We have plotted the dominant component of the  $5q_u$  and  $4e_{2u}$  relativistic molecular orbitals (the partners of the nonrelativistic  $t_{1u}$  orbital). These are shown in Fig. 2, where the  $\sigma$ - $\pi$   $3p$ -ligand mixing through the protactinium  $5f$  orbitals can clearly be seen. This additional  $5f$  character is found to be distributed across the ligand valence band, in con-

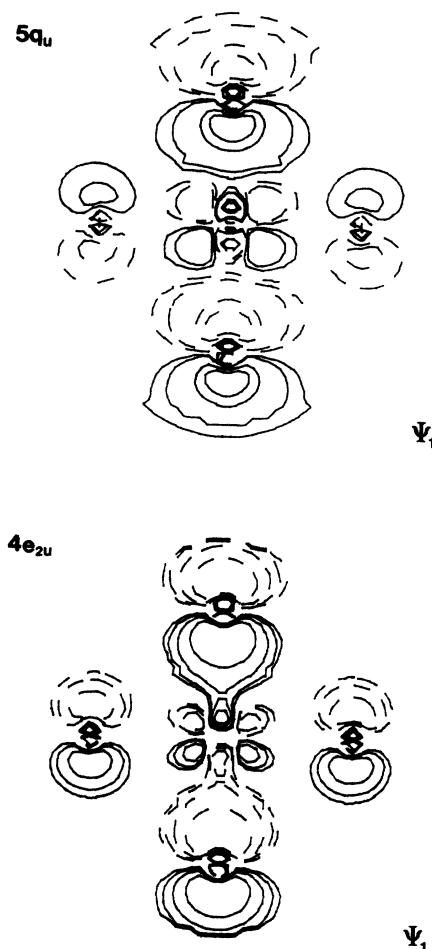


FIG. 2. Contours of the dominant component of the  $5q_u$  and  $4e_{2u}$  relativistic molecular orbitals. Contour values in  $(\text{electron}/\text{bohr}^3)^{1/2}$  are between  $\pm 0.2$  and  $\pm 0.002$ . Negative wave function contours are represented by dashed lines.

trast to crystal-field models. The  $5q_u$  orbital exhibits  $\pi$ -antibonding and limited  $\sigma$ -bonding character, while the  $4e_{2u}$  orbital has both  $\sigma$ - and  $\pi$ -bonding character.

An energy-level diagram of the  $\text{Pa}^{4+}$  ion in the  $\text{Cs}_2\text{ZrCl}_6$  lattice is shown schematically in Fig. 3. The NRL calculation produces a splitting of the seven  $5f$  orbitals into one orbital singlet ( $a_2$ ) and two triplets ( $t_2, t_1$ ), in agreement with previous quasirelativistic calculations.<sup>21</sup> In contrast, the relativistic calculation (DSW), which includes both crystal-field and spin-orbit effects, produces a low-lying Kramers doublet and two fourfold and two doublet orbitals, consistent with the observed infrared spectra.<sup>7</sup> From this diagram (Fig. 3) it is clearly noticed that in the absence of spin-orbit interactions, nonrelativistic or quasirelativistic theories produce an unrealistic description for the excited states of hexachloroprotactinate(IV). In a pure crystal-field treatment the eigenfunctions of the combined crystal-field and spin-orbit interactions are usually obtained in terms of chosen parameters: an atomic spin-orbit-coupling constant and crystal-field parameters. The usual procedure is first to diagonalize the crystal-field interaction for a

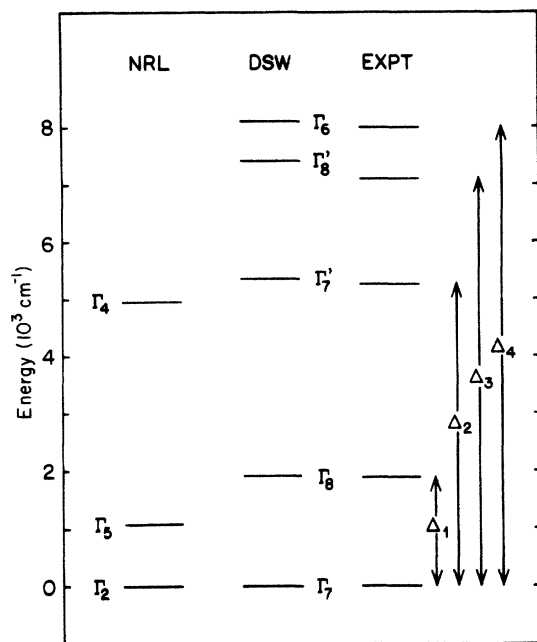


FIG. 3. Schematic energy-level diagram of the  $\text{Pa}^{4+}$  ion in the  $\text{Cs}_2\text{ZrCl}_6$  lattice. NRL: nonrelativistic limit splitting of the  $5f$  energy levels due to the octahedral crystal field. DSW: relativistic calculation which includes both crystal-field and spin-orbit interactions. Expt. observed infrared spectra, see Refs. 7 and 20.

spinless single  $f$  electron and then to include the spin-orbit interaction by adding spin functions to each of the orbital wave functions, and diagonalizing the spin-orbit Hamiltonian in two steps.<sup>3,7,20</sup> In the present nonempirical relativistic treatment both crystal-field and spin-orbit splittings come directly from the SCF DSW calculation. The crystal-field model predicts a  $5f^1$  configuration for the  $\text{Pa}^{4+}$  ion, while the present relativistic calculations predict a configuration of  $5f^{2,1}$ , due to the additional  $5f$  character found in the ligand valence band. This is in line with other relativistic calculations on actinide complexes<sup>9,13,16-19</sup> and arises mainly from participation of metal orbitals with  $t_{1u}$  character in metal-ligand bonding orbitals.

A charge breakdown for the crystal-field-like molecular orbitals is given in Table I. The amount of  $f_{5/2}$ - $f_{7/2}$  mixing is small, but non-negligible, as is the participation of the  $\text{Pa } 7p$  orbitals. A small fraction of the charge distribution in these orbitals is associated with the chlorine atoms, and is responsible for the ligand hyperfine splittings. Figure 3 defines the crystal-field splitting parameters, and the calculated and experimental values are collected in Table II. All the calculated splittings are slightly larger than those observed experimentally. It is well known that these splittings are determined by covalency effects.<sup>1,2,16,19</sup> It is probable that the present calculation slightly overestimates the amount of metal-ligand covalency; however, the calculated values are in very close agreement with experiment.

### B. Spin distributions and magnetic resonance parameters

In the present spin-restricted calculations, all of the spin density arises from the highest occupied orbital. Table III gives the populations for the partially occupied orbital from the two DSW calculations, and for comparison, from the analogous nonrelativistic  $a_{2u}$  orbital. The orbital characters are reported in terms of a Pauli description consisting of spherical harmonics multiplied by spin functions. The Pauli form was obtained from the DSW result by neglecting the third and fourth (small) components and assuming that the radial functions are the same in the two large components. In the nonrelativistic limit pure spin states are obtained (as required by symmetry), and one measure of the extent of spin-orbit mixing is the amount of minority spin mixed into the relativistic orbital. The analysis shows that the relativistic orbital is 66% spin up and 34% spin down. Thus, the excess of spin-up over spin-down population is 1.0 in the nonrelativistic wave function but only 0.32 in the relativistic one. This striking difference between the nonrelativistic and relativistic orbitals will have important consequences in the calculation and interpretation of the hyperfine splittings, as discussed below.

In nonrelativistic or quasirelativistic theories, there can be no chlorine  $s$  or  $p$  character in an orbital of  $a_{2u}$  symmetry, but there is about 0.5% chlorine  $d$ —orbital participation, so that the resulting orbital has about 99.5%  $\text{Pa } 5f$  character. In the relativistic case, the chlorine  $p_{3/2}$  orbitals are allowed to mix by double point-group symmetry, and the resulting orbital has about 1.4% chlorine  $p_{3/2}$  character and about 2%  $d_{5/2}$  character. The large contributions from the chlorine  $3d$  orbitals appear to be a relativistic effect. The contributions of the chlorine  $d$  orbitals are larger by a factor of 3 than those calculated for fluorine in the isoelectronic  $\text{NpF}_6$  complex.<sup>19</sup> The amount of covalency in  $\text{NpF}_6$  was determined to be  $\sim 5\%$  (from fluorine  $2p_{3/2}$  orbitals),<sup>19</sup> while the amount of covalency in  $\text{PaCl}_6^{2-}$  is predicted to be  $\sim 3\%$  (2% from the chlorine  $3d$  orbitals). As can be seen from Table III, the charge distribution in the partially occupied orbital is nearly the same in the two DSW calculations (using Slater's and the relativistic exchange-correlation potential). These small charge differences would have a negligible effect on the calculated spin-dependent properties.

The paramagnetic resonance and electron-nuclear double-resonance spectra for  $^{231}\text{Pa}$  in a single crystal of  $\text{Cs}_2\text{ZrCl}_6$  have been reported by Axe *et al.*,<sup>6,7</sup> and the experimental findings have been reviewed by Abragam and Bleaney<sup>1</sup> and by Boatner and Abraham.<sup>2</sup> In this host crystal the  $\text{PaCl}_6^{2-}$  unit shows very small distortions from octahedral symmetry, so that the observed  $g$  and metal hyperfine ( $A$ ) tensors are isotropic.<sup>6,7</sup>

Our method for calculating molecular  $g$  tensors and hyperfine interactions has been described earlier<sup>33-38</sup> and is based upon a first-order perturbation to the Dirac Hamiltonian so that the effects of magnetic fields are described by the perturbation operator  $\mathcal{H}_1$ ,

$$\mathcal{H}_1 = e\boldsymbol{\alpha} \cdot \mathbf{A}, \quad (1)$$

where  $\boldsymbol{\alpha}$  is the vector of  $4 \times 4$  Dirac matrices and  $\mathbf{A}$  is the

TABLE I. Analysis of the crystal-field orbitals. Asterisks indicate symmetry-folding contributions.

Level	$-E$ (eV)	Pa					Cl				
		$p_{1/2}$	$p_{3/2}$	$f_{5/2}$	$f_{7/2}$	$s_{1/2}$	$p_{1/2}$	$p_{3/2}$	$d_{3/2}$	$d_{5/2}$	
$5e_{2u}$	2.08	1.0	*	*	86.4	0.0	4.8	0.6	7.2	0.0	
$7q_u$	2.17	*	0.5	3.4	85.9	0.0	1.2	3.0	3.0	3.0	
$3e_{3u}$	2.36	*	*	0.5	95.9	*	*	1.2	0.6	1.8	
$6q_u$	2.85	*	0.4	84.8	5.6	0.0	0.0	4.8	0.0	4.4	
$2e_{3u}$	3.09 <sup>a</sup>	*	*	95.9	0.7	*	*	1.4	0.0	2.0	

<sup>a</sup>Highest occupied molecular orbital.

electromagnetic vector potential. For the Zeeman interaction  $\mathbf{A} = \frac{1}{2}(\mathbf{B} \times \mathbf{r})$ , where  $\mathbf{B}$  is the external magnetic field. For the hyperfine interaction  $\mathbf{A} = (\boldsymbol{\mu} \times \mathbf{r})/r^3$ , where  $\boldsymbol{\mu}$  is the nuclear magnetic moment. Matrix elements of these operators are evaluated in the basis spanning the two rows of the  $e_{3u}$  representation of the partially occupied orbital. The details of the evaluation of the angular and radial integrals have been described elsewhere.<sup>33,34</sup> The resulting perturbation energies are then fitted to the usual spin Hamiltonian:

$$\mathcal{H}_{\text{spin}} = \mathbf{S}' \cdot \mathbf{g} \cdot \mathbf{B} + \mathbf{S} \cdot \mathbf{A}_n \cdot \mathbf{I}_n, \quad (2)$$

where a value of  $\mathbf{S}' = \frac{1}{2}$  is used to describe the ground-state Kramers doublet,  $\mathbf{I}_n$  is a nuclear-spin operator, and  $n = \text{Pa}$  or  $\text{Cl}$ . This relativistic first-order perturbation scheme has been shown to be successful in calculating magnetic resonance parameters for heavy diatomic radicals,<sup>33</sup> transition metal,<sup>35</sup> lanthanide,<sup>34</sup> and actinide<sup>19</sup> complexes, as well as in low-nuclearity gold and silver clusters.<sup>36–38</sup>

A noticeable difference between crystal-field theory and the present calculations is that we retain all four components of the Dirac equation, and our Zeeman and hyperfine perturbations are given by Eq. (1). Hence, we do not need matrix elements of  $\mathbf{L}$  or  $\mathbf{S}$ , but rather of  $(\boldsymbol{\alpha} \times \mathbf{r})$ . Since  $\boldsymbol{\alpha}$  is a vector of off-diagonal matrices, these integrals connect the upper and lower components of the Dirac spinors.<sup>33,34</sup>

Table IV gives the results of the present calculations for magnetic resonance parameters. In reporting our results we will discuss our calculated values at the Pa—Cl distance of 2.62 Å using Slater's potential, since, as can be seen from Table IV, the use of the relativistic exchange-correlation potential or the calculated values at the shorter Pa—Cl distance of 2.52 Å does not lead to any significant difference. For the molecular  $g$  tensor, the

TABLE II. Crystal-field splittings. All values in  $\text{cm}^{-1}$ . See Fig. 3 for notation.

	DSW	Expt. <sup>a</sup>
$\Delta_1$	1920 (1935) <sup>b</sup>	1900
$\Delta_2$	5880 (5806) <sup>b</sup>	5215
$\Delta_3$	7429 (7420) <sup>b</sup>	7085
$\Delta_4$	8121 (8226) <sup>b</sup>	8000

<sup>a</sup>References 7 and 20.

<sup>b</sup>Transition-state calculations.

NRL calculation predicts a value of 1.967; however, it should yield a  $g$  tensor of exactly 2. This error of 1.6% may arise from numerical approximations used in evaluating the expectation values of the Zeeman operator. In the absence of spin-orbit mixings, the  $\text{PaCl}_6^{2-}$  molecule, which has a single unpaired  $f$  electron, will exhibit resonances at the spin-only value. However, this molecule is characterized by an isotropic  $g$  tensor of  $-1.142$ , far from the nonrelativistic limit. In other studies we have found that the difference between the DSW and NRL calculations is often a good approximation to  $\Delta g = g - g_e$ .<sup>19,36</sup> These calculations are shown in Table IV. Fairly good agreement between the calculated and experimental values of  $\Delta g$  exists. Since  $\Delta g$  is very large in this complex, the uncorrected DWS results are reasonably accurate, indicating that the molecular wave function has the correct behavior. Crystal-field arguments indicate that the  $g$  tensor should be negative with a theoretical value of  $-1.428$  for a doublet with no crystal-field admixture from excited states. The DSW results show unambiguously that the  $g$  tensor for the relativistic state has the opposite sign from the nonrelativistic state.

TABLE III. Spin populations in terms of Pauli decomposition, see text.

	$l$	$m$	Spin	Population
Nonrelativistic <sup>a</sup>				
Pa	$f$	$-2$	$\alpha$	0.497
	$f$	$2$	$\alpha$	0.497
Cl	$d$	$-2$	$\alpha$	0.002
	$d$	$2$	$\alpha$	0.002
Relativistic <sup>b</sup> ( $2e_{3u}$ )				
Pa	$f$	$-2$	$\alpha$	0.606 (0.606) <sup>c</sup>
	$f$	$-1$	$\beta$	0.195 (0.193) <sup>c</sup>
	$f$	$2$	$\alpha$	0.048 (0.050) <sup>c</sup>
Cl	$p$	$-1$	$\beta$	0.014 (0.014) <sup>c</sup>
	$d$	$-2$	$\alpha$	0.005 (0.005) <sup>c</sup>
	$d$	$-1$	$\beta$	0.014 (0.015) <sup>c</sup>
	$d$	$2$	$\alpha$	0.001 (0.001) <sup>c</sup>

<sup>a</sup> $c = \infty$ .

<sup>b</sup> $c = \alpha^{-1}$ , where  $\alpha$  is the fine-structure constant.

<sup>c</sup>Values are for a relativistic exchange-correlation potential, see text.

TABLE IV. Magnetic resonance parameters. Results A and B use Slater's exchange potential. Values in parentheses use the relativistic exchange potential of Refs. 30 and 31.  $d(\text{Pa}-\text{Cl})=2.52 \text{ \AA}$  (A) and  $2.62 \text{ \AA}$  (B).

		A	B
Molecular $g$ tensor			
	$c = \infty$	1.952	1.967(1.956)
	$c = \alpha^{-1}$	-1.185	-1.226 (-1.217)
	Expt. <sup>a</sup>	-1.142	
Calc.	$\Delta g \sim (g - g_e)$	-3.137	-3.193 (-3.173)
Expt.	$\Delta g = (g - g_e)$	-3.144	
Hyperfine tensors (MHz)			
<sup>231</sup> Pa	$c = \alpha^{-1}$	-1410	-1438 (-1428)
	Expt. <sup>a</sup>	-1578	
<sup>35</sup> Cl	$c = \alpha^{-1}$		
	for $a_{\parallel}$	-2.3	-2.2 (-2.2)
	for $a_{\perp}$	0.0	0.0 (0.0)

<sup>a</sup>References 6 and 7.

For the <sup>231</sup>Pa hyperfine interaction, Table IV shows that the DSW calculations predict a large negative isotropic tensor in close agreement with the experimental value.<sup>7</sup> In the nonrelativistic limit ( $c = \infty$ ), both the Fermi-contact and spin-dipolar contributions to the <sup>231</sup>Pa hyperfine tensor vanish by symmetry. The DSW calculated tensors are accurate to within 8%. The relatively close agreement between theory and experiment suggests that core spin-polarization effects (not included in these calculations) are fairly small, in agreement with the analysis of Axe *et al.*<sup>7</sup> This is in contrast to the situation in transition-metal complexes, where core-polarization effects are a major contribution to the observed hyperfine interactions.<sup>39,40</sup> All of the relativistic ( $c = \alpha^{-1}$ ) value comes from the "orbital term" which arises from unquenched orbital angular momentum, since the spin-dipolar and Fermi-contact contributions vanish by symmetry.

Results for the chlorine hyperfine interactions are also given in Table IV. These are predicted to be anisotropic, but very small, consistent with the larger contributions from the  $d_{5/2}$  spinors (2% versus 1.4% from the  $p_{3/2}$  spinors) to the partially occupied orbital. This is in contrast to the situation observed in NpF<sub>6</sub> where the DSW calculations predict a value of -56.1 MHz for the parallel component, due to the larger participation of the fluorine  $2p_{3/2}$  orbitals (about 5%).<sup>19</sup> The close agreement between theory and experiment for the crystal-field, Zeeman, and hyperfine splittings suggests that the predicted amount of covalency is likely to be correct.

#### IV. CONCLUSIONS

The calculations presented here represent the first application of the Dirac scattered-wave method to the study of the magnetic properties of protactinium complexes. The calculations predict that the unpaired electron spends about 3% of its time on the ligand and has about 2% chlorine  $3d_{5/2}$  character. Orbital contributions, which arise from unquenched orbital angular momentum, contribute significantly to the Zeeman effect, as well as to the <sup>231</sup>Pa hyperfine interactions. The calculations exhibited fairly good agreement with experimental crystal-field splittings and with the observed molecular  $g$  tensor and <sup>231</sup>Pa hyperfine interactions. Although this complex has a simple  $f^1$  configuration, a fairly complex relativistic (four-component) wave function is required to interpret correctly the available experimental data. The ability of the DSW model to provide a qualitative guide to the spectra and magnetic properties of actinide complexes has proved to be impressive, and argues well for its continued use for the elucidation of the electronic structure of molecules or clusters containing heavy atoms, in which relativistic effects are significant.

#### ACKNOWLEDGMENTS

We are grateful for financial support from Cray Research Inc. and the Robert A. Welch Foundation (Grant No. Y-743). Computing time was provided by the U.T. System Center for High Performance Computing.

<sup>1</sup>A. Abragam and B. Bleaney, *Electron Paramagnetic Resonance of Transition Metal Ions* (Clarendon, Oxford, 1971).

<sup>2</sup>L. A. Boatner and M. M. Abraham, *Rep. Prog. Phys.* **41**, 87 (1978).

<sup>3</sup>R. J. Elliot and K. W. H. Stevens, *Proc. R. Soc. (London)*, Ser. A **218**, 553 (1953).

<sup>4</sup>J. C. Eistenstein and M. H. L. Pryce, *Proc. R. Soc. (London)* Ser. A **255**, 181 (1960).

<sup>5</sup>B. R. McGarvey, in *Organometallics of the f Elements*, edited by J. J. Marks and R. D. Fischer (Reidel, Dordrecht, 1979).

<sup>6</sup>J. D. Axe, R. Kyi, and H. J. Stapleton, *J. Chem. Phys.* **32**, 1261 (1960).

<sup>7</sup>J. D. Axe, H. J. Stapleton, and C. D. Jeffries, *Phys. Rev.* **121**, 1630 (1961).

<sup>8</sup>P. Pyykkö, *Adv. Quantum Chem.* **11**, 353 (1978).

<sup>9</sup>D. E. Ellis, *Actinides in Perspective*, edited by N. M. Edelstein

(Pergamon, Oxford, 1982), p. 123.

<sup>10</sup>*Relativistic Effects in Atoms, Molecules, and Solids*, edited by G. L. Malli (Plenum, New York, 1983).

<sup>11</sup>K. Balasubramanian and K. S. Pitzer, *Adv. Chem. Phys.* **67**, 287 (1987).

<sup>12</sup>G. L. Malli, in *Molecules in Physics, Chemistry, and Biology*, edited by J. Maruani (Reidel, Dordrecht, 1988), Vol. II, pp. 85-144.

<sup>13</sup>P. J. Hay, W. R. Wadt, L. R. Kahn, R. C. Raffaneti, and D. H. Phillips, *J. Chem. Phys.* **71**, 1767 (1979).

<sup>14</sup>M. Boring and J. H. Wood, *J. Chem. Phys.* **71**, 392 (1979).

<sup>15</sup>J. E. Harriman, *Theoretical Foundations of Electron Spin Resonance* (Academic, New York, 1978).

<sup>16</sup>D. D. Koelling, D. E. Ellis, and R. J. Bartlett, *J. Chem. Phys.* **65**, 3331 (1976).

<sup>17</sup>D. E. Ellis, A. Rosen, and V. A. Gubanov, *J. Chem. Phys.* **77**,

- 4051 (1982).
- <sup>18</sup>D. A. Case and C. Y. Yang, *J. Chem. Phys.* **72**, 3443 (1980).
- <sup>19</sup>D. A. Case, *J. Chem. Phys.* **83**, 5792 (1985).
- <sup>20</sup>L. R. Raubenheimer, E. Boesman, and H. J. Stapleton, *Phys. Rev. A* **137**, 1449 (1965).
- <sup>21</sup>G. Thornton, N. Rösch, and N. M. Edelstein, *Inorg. Chem.* **19**, 1304 (1980).
- <sup>22</sup>C. Y. Yang and S. Rabii, *Phys. Rev. A* **12**, 362 (1975).
- <sup>23</sup>D. A. Case, *Annu. Rev. Phys. Chem.* **33**, 151 (1982).
- <sup>24</sup>C. Y. Yang, in *Relativistic Effects in Atoms, Molecules and Solids*, edited by G. L. Malli (Plenum, New York, 1983), p. 335.
- <sup>25</sup>C. Y. Yang and D. A. Case, in *Local Density Approximations in Quantum Chemistry and Solid State Physics*, edited by J. P. Dahl and J. Avery (Plenum, New York, 1984), p. 643.
- <sup>26</sup>J. G. Norman, Jr., *Mol. Phys.* **31**, 1191 (1976).
- <sup>27</sup>D. Brown, T. L. Hall, and P. T. Moseley, *J. Chem. Soc. Dalton Trans.* **686**, (1973).
- <sup>28</sup>D. Brown, C. T. Reynolds, P. T. Moseley, *J. Chem. Soc. Dalton Trans.* **857**, (1972).
- <sup>29</sup>J. C. Slater, *Quantum Theory of Molecules and Solids* (McGraw-Hill, New York, 1974), Vol. IV.
- <sup>30</sup>L. Hedin and B. I. Lundqvist, *J. Phys. C* **4**, 2064 (1974).
- <sup>31</sup>A. H. MacDonald and S. H. Vosko, *J. Phys. C* **12**, 2977 (1979).
- <sup>32</sup>M. P. Das, M. V. Ramana, and A. K. Rajagopal, *Phys. Rev. A* **22**, 9 (1980).
- <sup>33</sup>R. Arratia-Perez and D. A. Case, *J. Chem. Phys.* **79**, 4939 (1983).
- <sup>34</sup>D. A. Case and J. P. Lopez, *J. Chem. Phys.* **80**, 3270 (1984).
- <sup>35</sup>J. P. Lopez and D. A. Case, *J. Chem. Phys.* **81**, 4554 (1984).
- <sup>36</sup>R. Arratia-Perez and G. L. Malli, *J. Chem. Phys.* **84**, 5891 (1986).
- <sup>37</sup>R. Arratia-Perez and G. L. Malli, *J. Chem. Phys.* **85**, 6610 (1986).
- <sup>38</sup>R. Arratia-Perez and G. L. Malli, *J. Magn. Reson.* **73**, 134 (1987).
- <sup>39</sup>R. Arratia-Perez and F. U. Axe, and D. S. Marynick, *J. Phys. Chem.* **91**, 5177 (1987).
- <sup>40</sup>R. Arratia-Perez and D. S. Marynick, *J. Chem. Phys.* **87**, 4644 (1987).